Enhancing offshore service vessel concept design by involving seakeeping: developing a framework to efficiently design high performance offshore service vessel concepts

Bronkhorst, P.; Winter, R. de; Velner, T.; Kana, A.A.

Enhancing Offshore Service Vessel Concept Design by Involving Seakeeping - Developing a Framework to Efficiently Design High-Performance Offshore Service Vessel Concepts

Philip Bronkhorst, BW Offshore, Oslo/Norway, philip.bronkhorst@bwoffshore.com
Roy de Winter, C-Job Naval Architects, Hoofddorp/The Netherlands, r.dewinter@c-job.com
Thijs Velner, C-Job Naval Architects, Rotterdam/The Netherlands, t.velner@c-job.com
Austin A. Kana, Delft University of Technology, Delft, The Netherlands, a.a.kana@tudelft.nl

Abstract

This paper describes a design framework to efficiently design high-performing Offshore Service Vessel (OSV) concept designs incorporating seakeeping. The proposed framework optimizes the main particulars and length of different hull sections to maximize performance for key performance indicators (KPIs), including ship resistance, lightship weight, and seakeeping. For this work, sea-keeping performance is measured by the Operability Robustness Index (ORI), which considers the area of operation, motion limits, and motion characteristics. An initial stability constraint ensures feasibility. The framework generates a Pareto-frontier showing the trade-offs between KPIs and the corresponding variable combinations. A case study is performed to validate the framework. Comparing the Pareto-optimal solutions with the existing baseline concept design, the ORI can be increased up to 3.6%, the lightship weight decreased by 21.1% and the ship resistance decreased by 13.0%.

1. Introduction

The growth in the offshore wind industry has increased demand for offshore service vessels (OSVs), *Loos et al. (2020)*. These vessels often operate in harsh conditions, and many feature motion-compensated equipment. Consequently, their performance is heavily dependent on their seakeeping characteristics. Conventional ship design processes fail to effectively consider seakeeping early in the design process. This leads to the potential of suboptimal vessel designs. To design high-performing OSVs efficiently, there is a need for ship design methods that consider seakeeping effectively early in the design process. In recent years, C-Job has been developing the Accelerated Concept Design methodology (ACD) *De Winter et al. (2020)*. In the ACD framework, efficient global optimization algorithms are linked to a parametric modeling environment. The ACD framework is implemented in the NAPA software (Naval Architectural Package). Utilizing the NAPA environment and the ACD optimization philosophy, a framework is developed to effectively consider the seakeeping behavior as an optimization objective amongst other relevant, mostly conflicting design objectives such as costs, weights, and resistance. This design methodology is also considered a 'holistic' design method.

2. Gap Analysis

2.1. The conventional ship design process

Ship design is a complex multifaceted problem, requiring the integration of many engineering disciplines. The end goal is to design a ship that can carry out its designated task, doing so in a cost-efficient way. Many design trade--offs exist, and compromises are made throughout the design process. 'A successful ship design is the result of good and close cooperation between the designer, the customer, the yard, and the equipment suppliers', *Vossen et al. (2013)*. In the last 70 years, many new developments have been introduced by academia and industry. These range from developing certain ship design processes, such as the design spiral, to more advanced design and calculation methods with the onset of computer--aided design (CAD). The former, known as the 'ship design spiral', is an iterative process whereby the ship design progresses towards a converged solution. In theory, following the design spiral allows for an ideal converged design solution. In practice, a ship design process tends to differ, which the spiral fails to capture, *Pawling et al. (2017)*. Shortcomings of the ship design spiral, noted by numerous research, are:

- The design spiral assumes various aspects of the ship design occur sequentially. In practice, during the design process, the time pressure forces simultaneous engineering of various aspects of the ship design. Some ship aspects, such as seakeeping and ship resistance, need to be considered simultaneously as they are principally intertwined.
- The design spiral assumes the iterative process leads to an ideal solution. Each step provides input to the consecutive step. As such, the initial design direction governs each consecutive step. Hence, the spiral constrains the design space rapidly. Rather than converging to an optimal design solution, the design spiral attempts to make the initial design direction 'work'.
- The design spiral was developed during a time when computers were in an infantile phase, *Nowacki (2010)*. This is reflected by the design spiral, as it only addresses design aspects that could be deducted at the time. Since the 2000s, computers can extensively assist naval architects in the design of ships. As such, contrary to making a certain design 'work', naval architects are more than ever enabled to find optimal design solutions.

To conclude these findings, the design spiral was created to enable naval architects to develop ships effectively without the use of computers. In the 21st century, computers can assess lots of ship variables simultaneously. This can enable naval architects to create high-performing vessel designs. To do so, holistic ship design methods have been developed.

2.2. Holistic design methods

Making the correct design decisions early in the design of a vessel is highly important yet challenging. To mitigate this challenge and facilitate the design of high-performing vessels the concept design phase should consider all relevant aspects to the vessel *Papanikolaou (2010)*, *Andrews (2017)*. The development of computing technology has enabled naval architects to approach ship design in such a manner regardless of the complexity, *Nowacki (2010)*. In the last decade, much effort has been made by academia to develop such design methods in the form of ship synthesis models, *Andrews (2017)*, *Nowacki (2010)*. These methods have started to gain traction by the industry and are typically called 'holistic' design approaches. Broadly speaking, these methods optimize a set of design variables to a set of design objectives by the means of various evaluation methods by an optimization\ algorithm in an iterative process. Additionally, the subsequent design must satisfy certain constraints. This (simplified) working principle is depicted in Fig.1.

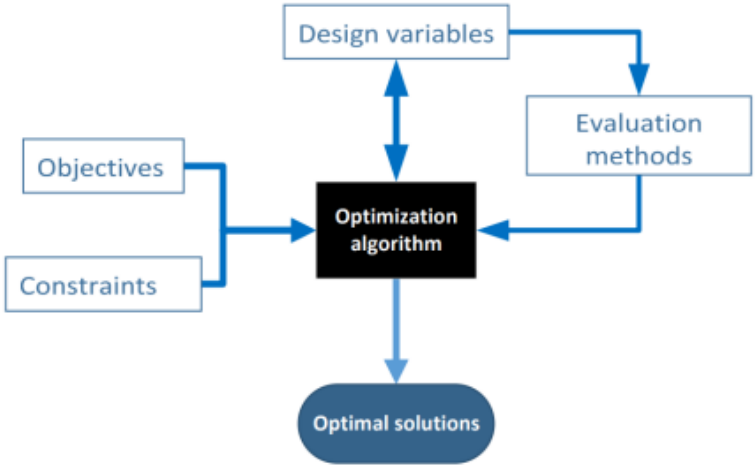

Fig.1: Holistic design method working principle

The outcome of the depicted procedure is a set of 'Pareto -optimal' solutions. These are design solutions on a Pareto- frontier, indicating the trade--offs between two or more design objectives. Naval architects can identify the exact trade--offs and determine optimal design solutions. These efforts have been extended to incorporate the estimation of various vessel aspects during the concept design phase, which

was previously only done in later design phases. C--Job's ACD method also concerns such an approach, as it can deal with conflicting objectives while dealing with physical and regulating authorities-imposed constraints, *De Winter et al. (2020)*. Thereby, the risk of having to do sub-optimal design 'work' is mitigated during contract and detail design. Ultimately, naval architects are given the freedom to choose a configuration that best suits the client's demands.

Applying the ACD method requires determining the design drivers and corresponding objectives, constraints, and parameters relevant to OSV design. Specific focus is given to parameters determined during concept design.

2.3. Design drivers

The design drivers are based on requirements for OSV types: Platform Supply Vessels (PSVs), Anchor Handling Tug Suppliers (AHTSs), Offshore Subsea Construction Vessels (OSCVs), and walk-to-work (W2W)-vessels. The design drivers and their corresponding objectives (key performance indicators), constraints parameters, and required design input are:

- Seakeeping capability - Ability to operate in harsh environments. Reflected by a measure of operability, the Operability Robustness Index (ORI), a robust indicator of seakeeping performance, *Gutch et al. (2017)*.
- Ship resistance - The ship resistance translates to power requirement and fuel costs. Hence, this objective forms a relative indication of OPEX to differentiate between different configurations, which forms an important design driver during concept design.
- Lightship weight - The lightship weight indicates the required materials and fabrication for a vessel. Thereby, the objective allows for weighing the CAPEX between different configurations.
- Vessel stability - The initial metacentric height of vessels is a measure of feasibility for vessels, as it is required to satisfy a minimum criterion.
- Vessel size - The size of the vessel may be bound by requirements to ensure suitable space for machinery, equipment, accommodation, and so forth. During concept design, the naval architect can indicate certain boundaries to the minimum or maximum values.

A framework has been developed taking into consideration the OSV design drivers. This will be discussed in the next section.

3. Method

In this section, it is described how the ACD framework has been extended such that all the OSV design drivers can be considered.

3.1. Used software

The framework has been developed using C-Job's optimization algorithm and a parametric modeling environment in the form of NAPA. NAPA provides an integrated development environment (IDE) as well as multiple software packages relevant to the design of vessels using the code 'NAPA Basic'. The framework has been developed within NAPA's IDE. Thereby, all input, output, and intermediate data are managed within the IDE. The Naval Architect is provided with a user interface (UI) for the management of all parameters and results.

3.2. Optimization algorithm

Section 2 indicated a parametric ship model linked to various evaluation methods can improve the efficiency of ship design. Critically, the parameters will need to be steered by an optimization algorithm to maximize the evaluated performance. In complex design problems, such as a ship design problem,

there is often no one ‘optimal’ design solution. Rather, the naval architect has to decide the best compromise between conflicting design requirements. For example, decreasing the beam of a ship might decrease ship resistance but increase the maximum roll motion. Thereby, the ship resistance is improved at the cost of seakeeping performance. To best decide the trade-off, the extremities of the design space must be fully explored. To do so, C-Job developed several efficient global optimization algorithms which are specifically designed to limit the number of expensive simulations while considering the entire objective and constraint space by making use of cheap surrogate functions.

The OSV design is optimized with the SAMO-COBRA algorithm, which is short for Self-Adaptive Multi-Objective Constrained Optimization by using Radial Basis Function Approximations, *De Winter et al. (2021)*. SAMO-COBRA starts with a small number of initial designs which are well spread among the parameter space. The initial designs are evaluated on the real objective and constraint functions in the NAPA software resulting in a set of parameters with their corresponding objective and constraint scores. These scores are used to train Radial Basis Functions (RBFs) which form an approximation of the true objective and constraint functions. Then in each iteration of the algorithm, SAMO-COBRA considers the entire design space by using the computationally cheap RBF approximations to search for new feasible Pareto-efficient solutions. The solution which scores the best in both objectives simultaneously while being feasible is selected for evaluation. A multi-objective performance measure that indicates if a solution is close to the Pareto front and encourages diversity among the Pareto frontier is the Hypervolume Indicator, *Riquelme (2015)*. The solution that leads to the highest predicted hypervolume is selected for evaluation on the computationally expensive functions in the NAPA software. The results from these functions are added to the set of parameter, objective, and constraint scores after which the RBFs are automatically updated. The search for new feasible Pareto-efficient solutions is continuous until the user is happy with the results or until a predefined limit like passed time or the total number of real function evaluations has been reached.

The result of the optimization algorithm is a set of incomparable evaluated solutions on the Pareto frontier which form the trade-off between the objectives. Each solution on the Pareto frontier is an optimal solution until the preferences of all stakeholders are known and a decision can be made on which vessel to take to the next design phase. An example of a classical trade-off that can often be found on the Pareto frontier of a ship design problem is Light Ship Weight versus Resistance at the design speed. A long and slender ship will have less resistance compared and a higher steel weight compared to a shorter and wider variant.

3.3. Framework

The general framework, Fig.2, can be divided into five parts, these are elaborated in the following:

1. Input parameters
   This part of the framework defines the minimum input required to the optimization to assess the identified design drivers. A base hull shape that is to be transformed is defined. The base hull can be created in Rhinoceros3D or other similar software and is imported as an IGS file. Additionally, parameters defining the initial bilge keel dimensions, motion-sensitive equipment, area of operation, and loading conditions are defined:
   - Bilge keel (BK) dimensions - The influence of a bilge keel is calculated according to Ikeda’s method. To do so, a base bilge keel height, moment arm, and bilge keel length, *Ikeda (2004)*. The dimensions are scaled according to the dimensions of each iteration.
   - Motion sensitive systems specification - This item defines the motion limits and location of motion-sensitive equipment. The location forms the input to the calculation of motion response on the location of the equipment (local RAOs). The motion limits in the form of motions, velocities, and accelerations form input to the ORI calculation.
   - Area of operation - The area of operation directly influences seakeeping performance. Parameters reflecting the area of operation and environment are defined. To calculate the ORI, ocean data such as the wave spectrum and scatter diagram are required. Both are calculated

following guidelines from *DNV (2010)*. Specifically, a Pierson-Moskowitz (PM) spectrum model and a two-parameter Weibull distribution for the scatter diagram are used. The framework automatically calculates the wave spectrums and scatter diagram based on the input parameters. Both the wave spectrums and scatter diagram provide input to the calculation of the seakeeping objective.

- Loading condition - To assess the vessel stability and total displacement, the operational loading condition is established. Specifically, the weight and VcG w.r.t. deck of the deck load and accommodation and the VcG of the hull and ballast w.r.t. the ship depth is defined. These parameters form input to the deadweight in the initial stability calculation and the draft for ship resistance and seakeeping performance.

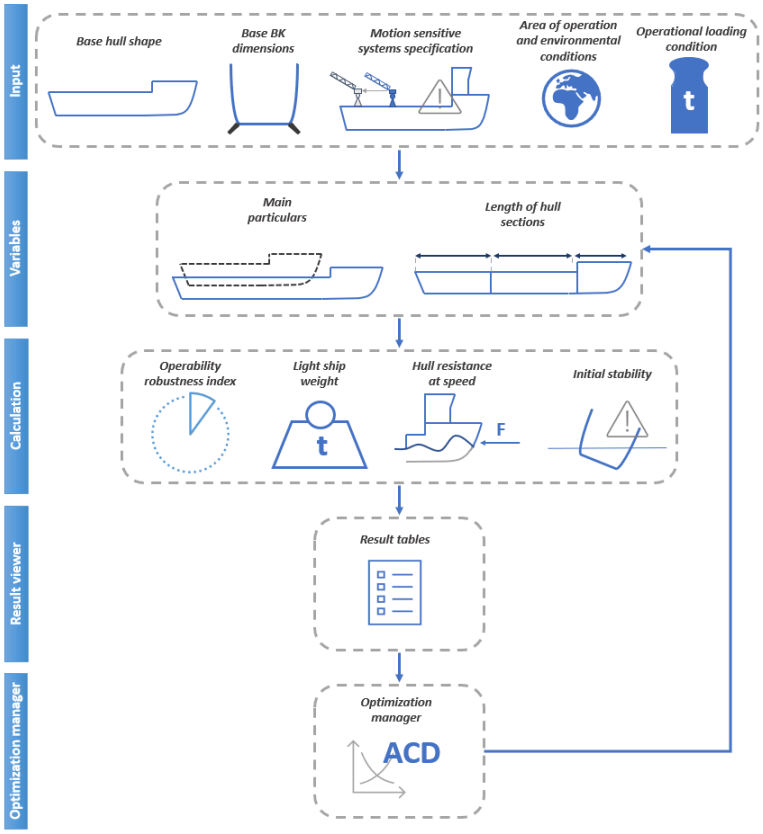

Fig.2: Framework

2. Design variables

In this section, the framework variables are defined. During an optimization run, these values are changed by the algorithm per iteration. If needed, a user can also input variables manually. Thereby, the global dimensions and front, aft, and global prismatic coefficients are varied. A description of each specific variable item is given below:

- Main particulars - The beam and draught are changed individually. The total length of the vessel is changed by varying the length of specific sections of the hull. Thereby, the length is defined as,

$$L_{tot} = L_{afts} + L_{mids} + L_{fwds}$$

L_{afts}, L_{mids}, and L_{fwds} are the aft-, mid-, and forward- section lengths of the hull. By changing these parameters, the aft-, mid-, and forward prismatic coefficients, L/B ratio, and L/D are adjusted. Alternative bow shapes, V/U-based sections, and finer hull shaping are not captured by this method.

- Length of hull sections - In this item, the aft-, mid-, and forward -section lengths of the hull are varied, which are summed to determine the total length of the ship. The variable length and beam form input to the hull form transformation method. The variable main particulars

form input to vessel reference dimensions, which are called upon for the ship resistance calculation and motion analysis. Based on the variables, the bilge keel moment arm and length are calculated, whereby,

$$RBILGE = \sqrt{VcB^2 + (0{,}5B)^2}$$

and,

$$LBILGE = L_{\text{mids}} \cdot \eta_{\text{LBILGE}}$$

$RBILGE$ is the moment arm, $LBILGE$ the length of the bilge keel. On some vessels, the bilge keel length may be slightly longer than the midship length to further increase roll damping. To account for this, a lengthening factor, $\eta L{-}bilge$, can be defined. The variables further form input to the calculation, which is discussed in the next subsection.

3. Calculation

This part of the framework performs all necessary calculations, following the predefined objectives and constraint functions. The variables form input to a freeform deformation (FFD) method. The FFD method transforms the base hull shape to an iteration-specific hull shape. Following the hull shape transformation, the ORI, lightship weight, initial stability, and ship resistance are calculated:

- Operability robustness index - The operability robustness index (ORI) forms a robust criterion to measure seakeeping performance developed by *Gutch et al. (2020)*. The ORI is based on the vessel RAOs, area of operation, and motion limits. RAOs are first calculated by NAPA's seakeeping application, which contains a strip theory formulation. As an input, area of operation, iteration specific hull shape, vessel loading condition draught and GM_T is used. Additionally, the radius of gyration is calculated as a factor of the length and width of the iteration. This factor is defined by the user and can be based on reference vessels. The roll damping factor is determined following Ikeda's method, which requires the length, height, and moment arm of the bilge keel. These dimensions are automatically scaled based on the iteration-specific ship dimensions. The full derivation of the ORI is given in the paper by *Gutch et al. (2020)*. To calculate the ORI requires **Error! Reference source not found.**the following calculation procedure: Based on the area of operation, as well as iteration specific hull shape, vessel loading condition draught and GM_T,

$$H_j(\omega;\beta) = \frac{s_j(\omega;\beta)}{\zeta(\omega)}$$

$H_j(\omega;\beta)$ is the RAO per DoF j, $s_j(\omega;\beta)$ the vessel response output signal which is partially dependent on wave frequency ω and wave angle β, and $\zeta(\omega)$ the wave excitation input signal. Once the RAOs have been calculated, the vessel response spectrum is calculated,

$$S_j(\omega;\beta;T_p) = |H_j(\omega;\beta)|^2 S_\zeta(\omega;T_p)$$

$S_\zeta(\omega; Tz; H_s)$ is the wave spectrum. The area enclosed by the spectrum forms a measure of variance (spread of vessel response), also known as the spectral moment m_n,

$$m_n(n;\beta;T_Z) = \int_0^\infty \omega^n \cdot S_j(\omega) \cdot d\omega$$

Depending on the value of n, the zeroth, first or second spectral moment is calculated. These represent the variance of response for motion, velocity, and acceleration, respectively. The root of this variance gives the standard deviation, σ_j,

$$\sigma_j(n;\beta;T_Z) = \sqrt{m_n(n;\beta;T_Z)}$$

which forms input to the tolerable significant wave height, $H_{s,\,tol}(n;\beta;Tz;\sigma_{j,\,tol})$ for a specific peak period, together with a particular motion limit $\sigma_{j,\,tol}$,

$$H_{s,tol}(n;\beta;T_Z;\sigma_{j,tol}) = \sigma_{j,tol}\frac{H_s}{\sigma_j(n;\beta;T_Z)}$$

The percentage operability is then calculated by comparing the evaluation of the scatter diagram. Specifically, evaluated is the percentage of the occurring waves that do not exceed the tolerable significant wave height. Hence, the total percentage operability is:

$$\text{PercOp}\left(n;\beta;\sigma_{j,tol}\right) = \frac{\sum f_{T_Z|H_S}\left(T_z \mid H_s \le H_{s,tol}\left(n;\beta;T_Z;\sigma_{j,tol}\right)\right)}{\sum f_{T_Z|H_S}(T_Z \mid H_S)}$$

As the percentage operability is determined for a range of motion limits up until the maximum motion limit (where the limit is $\sigma_{j,\,tol,\,max}$). The resultant data provides a curve showing percentage operability as a function of the motion limit. *Gutch et al. (2017)* only considered the ORI for a single motion, with constants n and β.

Considering $PercOp\ (\sigma_{j,\,tol})$, the ORI is calculated by integrating and normalizing the area under the curve,

$$ORI = \frac{\int_0^{max(\text{Percop})} \text{PercOp}\left(\sigma_{j,tol}\right) d(\text{PercOp})}{max(\text{PercOp}) \cdot 100}$$

The procedure above describes the calculation of tolerable significant wave height for an individual motion limit. *Gutch et al. (2017)* only considered a single limit in their research. However, to efficiently consider seakeeping, all limits should be considered. To do so, a modification is made to the calculation of the tolerable wave height, $H_{s,\,tol}$. This equation is evaluated for a range of motion limits of a specific DoF and type of motion. For example, for a maximum heave acceleration limit of $\ddot{z}_{i\,imit}$ of $1[m/s_2]$, percentage operability is evaluated for limits $\ddot{z}_{i\,imit}$ of $0.1, 0.2, 0.3, \ldots, 1.0[m/s_2]$. The number of steps in which the limit is varied is constant for each motion limit. For each 'step,' or percentage of the motion limits ($\%_{limit}$) the most stringent motion limit is critical and limiting to the operability of the ship. The critical motion limit results in the lowest tolerable wave height. Hence the calculation of ORI is expanded by evaluating for each step,

$$H_{s,tol}(\%_{limit},\beta;T_Z) = min\left(n;H_{s,tol}\left(\beta;T_Z;\sigma_{j,tol}\right)\right)$$

Thereby considering each motion limit. Once the tolerable wave height per limit step is known, the corresponding $PercOp\ (\beta;\%_{limit})$ is calculated. Finally, the ORI is evaluated:

$$ORI(\beta) = \int_0^{100\%} \text{PercOp}\ (\beta;\%_{\text{limit}})\, d(\text{PercOp})$$

- Lightship weight - This item estimates the lightship weight of the iteration. To calculate the lightship weight, the hull shape is estimated by the quadricubic number, *Aasen and Bjørhovde (2014)*.,

$$m_{ls} = \eta_{ls-contingency} \cdot k \cdot N_{qc}$$

m_{ls} is the lightship weight, k is a parameter determined based on a regression analysis of similar vessels from C-Job's reference vessel 'RefWeb.' $\eta_{ls-contingency}$ is a contingency factor, as there is still uncertainty involved (especially during concept design). N_{qc} is the quadricubic number which is calculated by,

$$N_{qc} = L^{4/3} \cdot B \cdot D^{1/2} \cdot \left(1 + \frac{3}{4}Cb\right)^{1/2}$$

This equation shows the differing influences of length, beam, draught, and block coefficient, for instance, length exponentially increases lightship weight due to a required increased bending stiffness and so forth, *Aasen and Bjørhovde (2014)*. This formulation was shown to provide good accuracy by multiple studies, *Ho et al. (2012)*.

- Initial stability - The initial stability in the form of transverse metacentric height (GM_T) is calculated. To begin, an estimate for KG is made by the following equation,

$$KG = \frac{KG_{ss}m_{ss} + KG_{dl}m_{dl} + KG_h m_h + KG_b m_b}{\sum m_i}$$

ss denotes the superstructure, dl the deck load, h the hull and b the ballast. The values for the superstructure and deck load form input to the calculation. The mass of the hull and the weight of the ballast is calculated by,

$$m_h = m_{ls} - m_{ss} - m_{dl}$$

and,

$$m_b = m_{\text{disp}} - m_{ls} - m_{\text{dl}}$$

The displacement weight, m_{disp}, is calculated by NAPA's hydrostatic calculation package for the iteration draught. The vertical center of gravity of both the hull and ballast are estimated based on a factor defined by the user. By subtracting KG from KM_T, an initial estimate for GM_T is obtained,

$$GM_T = KM_t - KG$$

KM_T is calculated by NAPA's hydrostatic calculation package.

- Ship resistance - To calculate the ship resistance, use is made of the NAPA Resistance and Propulsion manager application. This application provides a multitude of widely used empirical methods. Of these methods, Holtrop & Mennen is found to obtain accurate results for a wide range of vessels *(Holtrop et al. (1982))*, and a calculation package is available in NAPA. It should be noted that during the optimization, accuracy boundaries such as the L/B and B/T ratio ranges may be exceeded. At these extremities, Holtrop & Mennen is still able to calculate the ship resistance with limited accuracy. In these regions, the ship resistance calculation provides more of relative comparison between different variable combinations.

4. Result viewer
   This section provides the output of the calculation. These results are either used by the optimization to determine the variables for a new iteration or presented to the naval architect. The multi-dimensional Pareto frontier is presented, showing the trade-offs between objective scores. The actual optimum solution can further be deliberated by the naval architect when the relative importance of various design drivers is known.

5. Optimization manager
   This section manages the optimization. A user can select certain experiment settings and execute the optimization. Thereby, the user defines the variables with maximum and minimum values, objectives, constraints, and constraint values, constant values, and what components of the optimization to include.

4. Case study

4.1. Vessel introduction

The 'US Wind Feeder' is a vessel designed to support the construction and logistics of offshore wind farms in the United States. Specifically, the vessel allows non-American wind turbine installation vessels (WTIV) to construct wind farms in compliance with the Jones Act. To maximize operability, the vessel features a motion-compensated platform design by Ampelmann. Thereby, operability is a critical design driver, to enable a continuous supply of turbine components to the WTIV. The second design driver is costs- both CAPEX and OPEX. The vessel is part of a new business case proposing that maximizing WTIV's installation capability minimizes the building costs of a wind farm. Subsequently, the vessel's CAPEX -linked with the lightship weight is a critical component. Additionally, the CAPEX is interlinked with seakeeping performance. The Ampelmann platform forms a significant portion of the CAPEX - around 20% in the current concept - to realize high operability. Better seakeeping capabilities, lead to lesser requirements for the Ampelmann, improving its CAPEX. The ship's resistance is of lesser concern, as the wind farm site is close to shore. Based on the vessel's design philosophy, input to the optimization has been determined, which is given in the next section.

4.2. Optimization input

The optimization input has been determined together with C-Job naval architects. Three motion limit cases have been defined, following the locations shown in Fig.3. Motion limit case 1 concerns the motion-compensated Ampelmann platform. Motion limit case 2 concerns the risk of a turbine blade tip touching the water, which imposes a heave limit. Motion limit case 3 concerns a maximum amount of

blade accelerations, which the turbine blade can sustain. The corresponding exact limits and locations are given in Table I. Two loading conditions have been optimized. The heaviest operational loading condition, when the ship is fully loaded with turbine components, forms loading condition 1 (LC1). The lightest loading condition under which accelerations are important, which is when lifting the last item, forms loading condition 2 (LC2).

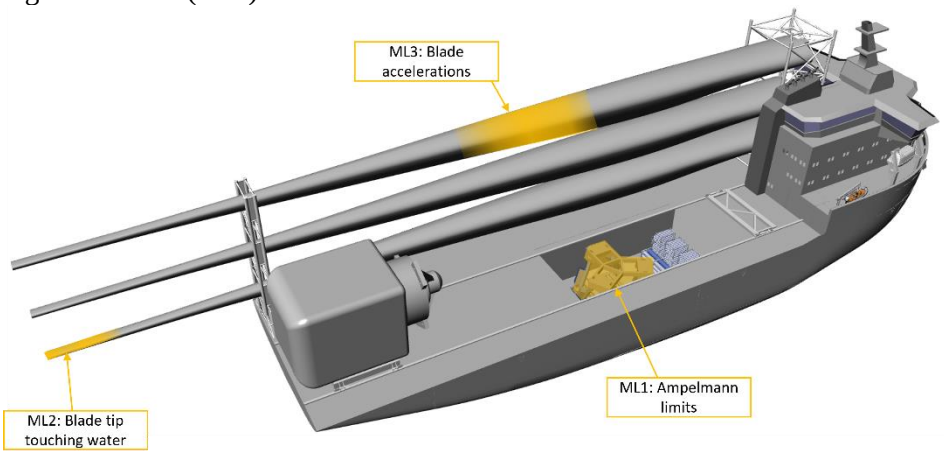

Fig.3: Motion limits case study

Table I: Optimization settings

Input

Input	*Symbol*	*Setting/specification/value*	*Unit*
Area	-	23, North Atlantic Ocean, East Coast USA	-
Hull shape	-	US Wind Feeder concept	-
Angle incoming waves	α_{RAO}	30.0	°
Motion sensitive equipment	-	Case 1: Ampelmann platform, near CoB Case 2: Lifting operation Case 3: End of blade tip	-
Loading condition	-	Condition 1: Maximum loading condition Condition 2: Lifting last item	-

Variables

Variables	*Symbol*	*Lower limit*	*Upper limit*	*Unit*
Aftship length	L_{afts}	30.0	50.0	m
Midship length	L_{mids}	10.0	40.0	m
Forwardship length	L_{fwds}	30.0	50.0	m
Beam	B	17.0	28.0	m
Draught	T	4.5	7.5	m

Constraints

Constraints	*Symbol*	*Lower limit*	*Upper limit*	*Unit*
Metacentric height	GM_T	2.0	-	m
Total length	L_{tot}	90.0	-	%

Objectives

Objectives	*Symbol*	*Unit*
ORI	ORI	–
lightship weight	LSW	t
Ship resistance	SR	kN

Algorithm settings

Item	*Setting*	*Unit*
Algorithm	SAMOCOBRA	–
Maximum iterations	300	#

5. Results

5.1. General results

Six optimization runs have been completed, each varying in either motion limit case or loading condition. The Pareto frontier has been found for all optimization runs as seen by the progression in hypervolumes in Fig.5, which all converge to an asymptote. Fig.4 shows each optimization's asymptote converging at a different value. As described in section 3.2 a higher hypervolume implies better objective scores.

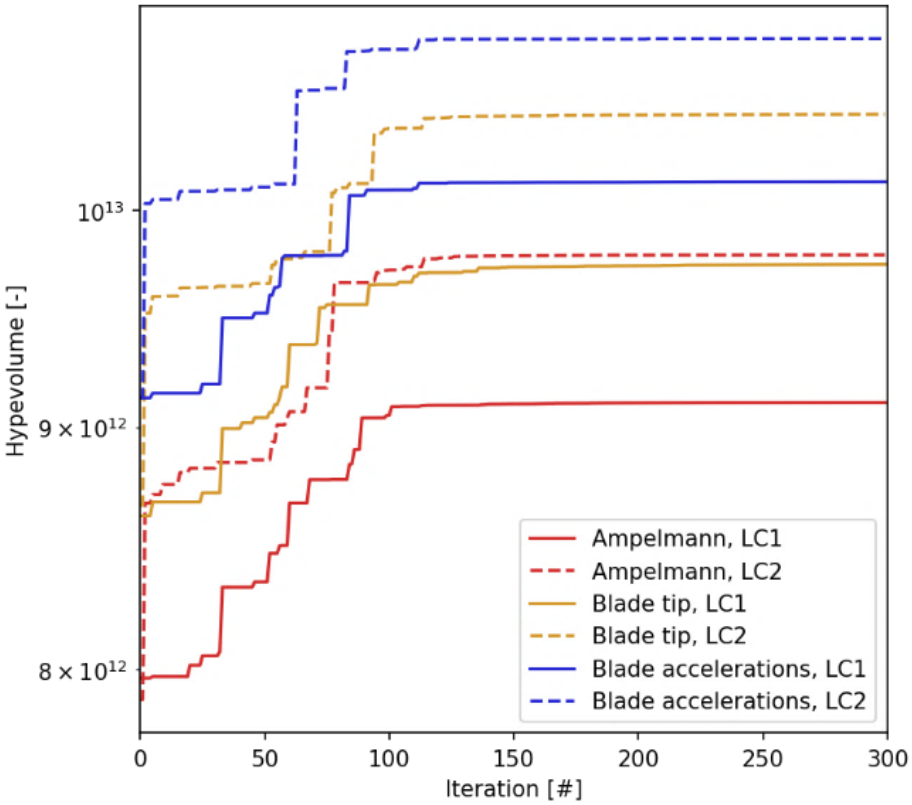

Fig.4: Hypervolume progression for six case study optimization runs

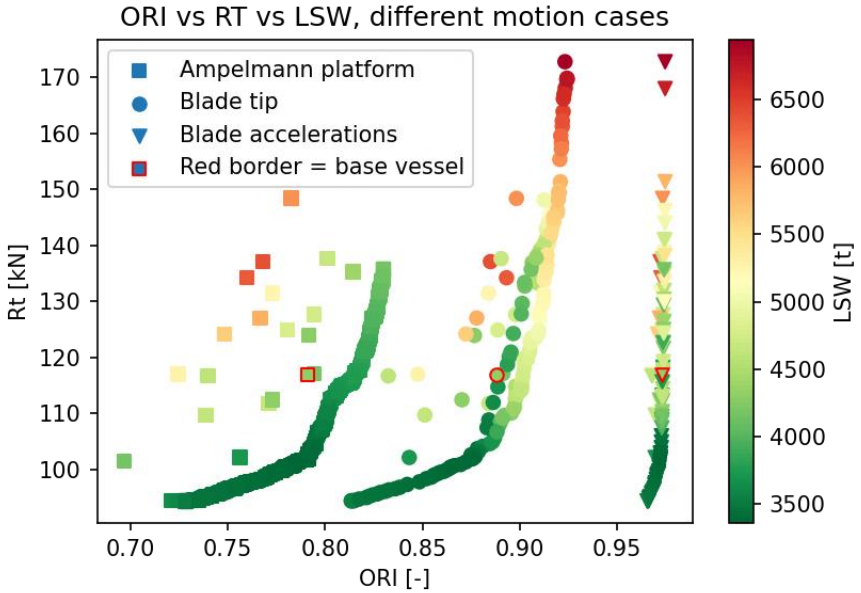

Fig.5: Optimization results for different motion limit cases

Fig.5 shows the Pareto frontiers of three different motion cases for one loading condition. All three Pareto frontier show better performance scores compared to the original solution. The highest combined objective scores are found when optimizing for the blade accelerations, followed by blade tip motions and the Ampelmann platform. Thereby, the Ampelmann platform forms the constraining motion limit case and will be further optimized upon in the study.

The effect of the two loading conditions (LC1 and LC2) becomes apparent when comparing the corresponding Pareto-frontiers in Fig.6.

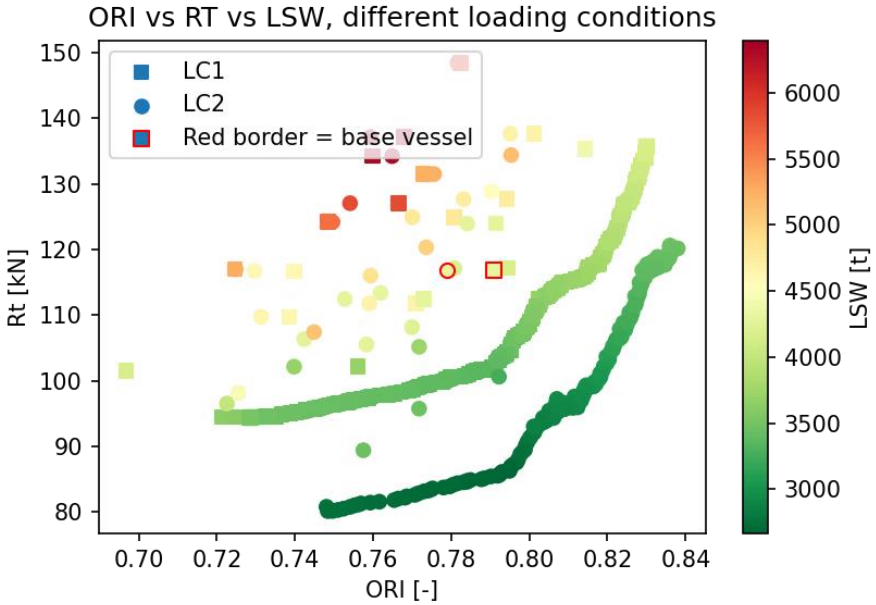

Fig.6: Optimization results for different loading conditions, with Ampelmann motion limits

Fig.6 shows LC2 allows for lower ship resistance and slightly lower lightship weight, whilst maintaining the same ORI value compared to that of LC1. LC2 allows for a slenderer vessel to satisfy the GMT constraint of 2 m, specifically vessels of around 19 m wide. The GMT constraint is satisfied for vessels at least 23 m wide for LC1. These slender vessels will not be feasible for LC1. Hence, LC1 is the critical loading condition. Together with the motion limits of the Ampelmann platform, which govern the maximum attainable seakeeping performance, this forms the critical vessel condition. In the next section, the results for this vessel condition will be further deliberated.

5.2. Analysis on critical vessel condition

The correlations between variables, feasible solutions, and high objective scores, can be illustrated by a parallel coordinate. Fig.7 shows the parallel coordinate plot of the results of the US Wind Feeder in critical condition for limiting motion cases 1 and LC1. In this plot, variable combinations have been scaled according to the ORI value. Per objective, the following correlations can be observed:

- Correlations between ORI value and variables - The resulting ORI value spans between 0.75[−] and 0.85[−]. All associated percentage operability values are quite high. A long aft ship and short forwardship, together with a high draught show to result in an ORI value. The parallel coordinate plot shows a trend of ships with short mid- and forwardship, and long aft ship attaining a high ORI value. The overall length is shown to be between 90 and 105 m, showing shorter vessels can attain a high ORI. The beam is adjusted to result in an initial GMT of 2 m, which reduced roll accelerations and allows for a high ORI value. This indicates that the Ampelmann platform's acceleration limits govern the seakeeping performance. Additionally, a higher block coefficient (CB) corresponds to a high ORI value.

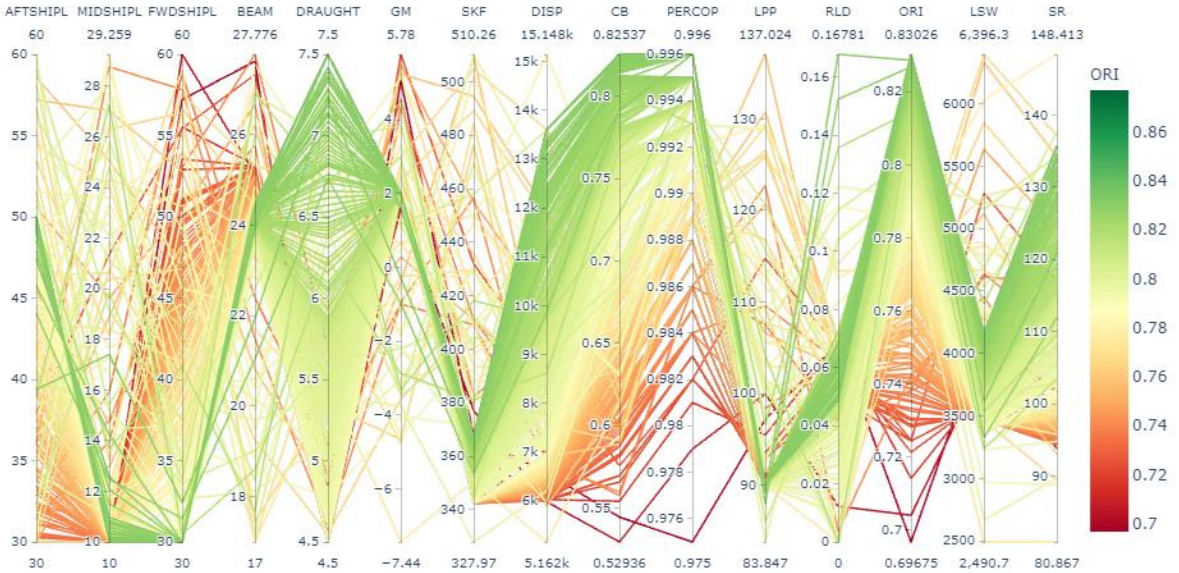

Fig.7: Parallel coordinate plot for US Wind Feeder case, LC1 and Ampelmann motion limits

- Correlations between initial stability and variables – Fig.7 shows how the optimization steers variable combinations towards a GMT of 2 m, as this allows a high ORI score. Consequently, this results in an inverse relationship between the draught and the beam. A slenderer beam requires the draught to be higher to satisfy the GMT constraint, and vice versa.
- Correlations between lightship weight and variables - A direct and positive correlation exists between length, beam, draught, and block coefficient. This is seen in the parallel coordinate plot. Additionally, most of the results have an LSW between 3500-4300 t, due to the relative shortness of Pareto-optimal vessels. The vessels with a higher ORI are seen to have a higher lightship weight, due to having a higher draught and block coefficient, hence a trade-off exists between ship resistance and draught.
- Correlations between ship resistance and variables - The ship resistance is seen to vary between 95-130 kN for most results. Shorter aft ship and longer forward ship lead to a lower ship resistance. The draught is seen to have an inverse relationship with ship resistance. Vessels with a deeper draught may be slenderer whilst satisfying the GMT, though it is not seen to result in a lower ship resistance. The adverse effects of a higher draught supersede the positive effects of a lower beam on ship resistance. The vessels with a higher ORI are seen to have a higher ship resistance, due to having a higher draught and block coefficient, hence a trade-off exists between ship resistance and ORI.

The framework does not provide one singular optimal solution. Rather, it provides insight into the combination of variables resulting in 'optimal solutions', solutions that maximize performance into one objective for a certain value for another objective. These results are shown in a Pareto-front in the next subsection. Additionally, these attainable values are compared to the current US Wind Feeder concept of C-Job.

5.3. Comparison with base vessel

Fig.8 shows the detailed optimization results with the Pareto-frontier. When compared with the current concept design, annotated as 'base design', all Pareto-optimal solutions show an improvement over the base design in lightship weight. Additionally, some Pareto-solutions show improvements in both ORI, ship resistance, and lightship weight. The solution with the same ORI but improving the ship resistance and lightship weight has been highlighted, as well as the solution with a similar ship resistance but improved ORI and lightship weight. The extremes of the Pareto-frontier are also annotated. Table II shows corresponding variables, KPI scores, and other parameters of these design solutions.

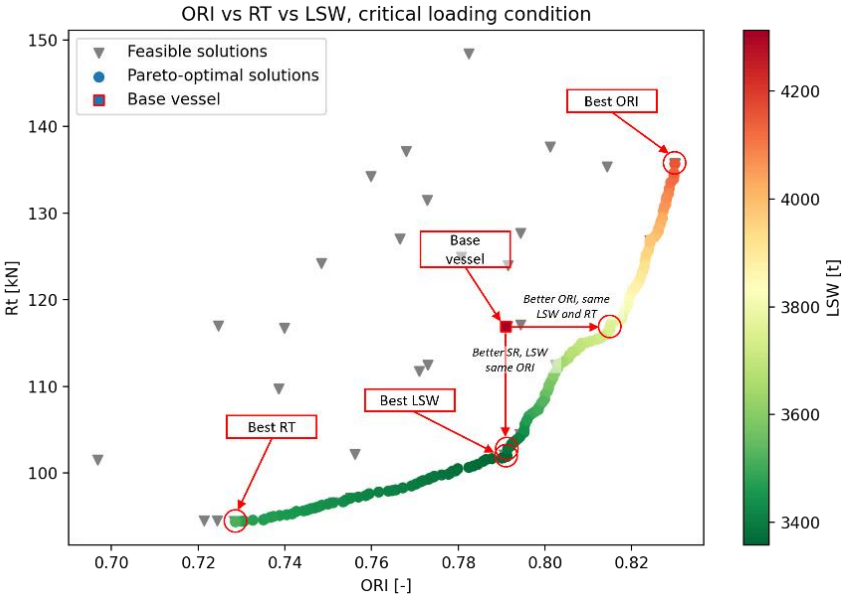

Fig.8: Detailed Pareto-frontier of case study, LC1, and Ampelmann motion limits

Table II: Overview of specific results of optimization for US Wind Feeder case study

Results of optimization for US Wind Feeder concept - critical condition								
Variables	*Symbol*	*Value*	*Value*	*Value*	*Value*	*Value*	*Value*	*Unit*
Solution	–	**Base vessel**	**Same RT. better ORI and LSW**	**Same ORI. better RT and LSW**	**Best ORI**	**Best LSW**	**Best RT**	–
Aftship length	L_{afts}	46.00	50.00	49.25	49.80	50.00	30.00	m
Midship length	L_{mids}	23.00	10.00	10.4	10.20	10.00	10.00	m
Forwardship length	L_{fwds}	34.50	30.00	30.35	30.00	30.00	50.835	m
Beam	B	23.80	23.99	23.6	24.22	23.48	25.26	m
Draught	T	5.50	5.98	4.5	7.50	4.50	4.50	m
Block coefficient	C_B	0.72	0.78	0.72	0.83	0.73	0.58	–
Metacentric height	GM_T	2.18	2.00	2.00	2.00	2.00	2.00	m
Stationkeeping force	SKF	398.78	354.70	342.38	367.44	342.38	342.36	kN
Operability robustness index	ORI	0.791	0.815	0.791	0.830	0.791	0.729	–
Difference ORI w.r.t. base vessel	-	-	3.03	0.00	3.55	0.00	-7.84	%
Percentage Operability	$PercOp$	99.2	99.4	99.2	99.6	99.2	98.3	%
Lightship weight	LSW	4310	3760	3450	3880	3360	3510	t
Difference LSW w.r.t. base vessel	-	-	-12.76	-21.14	-9.98	-22.04	-18.56	%
Ship resistance	R_T	116.93	116.90	101.79	135.69	101.91	96.36	kN
Difference R_T w.r.t. base vessel	-	-	-0.03	-12.95	16.04	-12.85	-17.49	%

Below, improvements in objectives are further elaborated:

- Improvements in ORI - The ORI shows to be improved up to 3.6%, depending on the combination of variables. The ORI is improved over the base vessel by increasing the aft ship length, draught, and subsequently the block coefficient, thereby keeping GMT at 2.0 m. The design solution with the highest ORI also shows a minor improvement in operability, namely 99.6% over 99.2% This does show that the base vessel should already allow for good year-round operability. The solutions offering the lowest lightship weight and ship resistance do so by minimizing draught. The vessel with the best ORI has an estimated lightship weight of 16.0% than that of the base vessel. The vessel with the lowest ship resistance shows a decrease of −7.8% in ORI. Hence, a trade-off exists between lightship weight and ship resistance. Though the ORI is only marginally improved, the framework can show that other performance criteria could significantly be optimized whilst maintaining seakeeping performance. Thereby, the naval architect might pursue extreme design solutions, which it would normally not dare to do so.
- Improvements in lightship weight - Design solutions close to the Pareto frontier allow for a reduction in lightship weight between 12.8% and 22.0%. The framework results showed that

shorter vessels (length = 90 m) can attain good seakeeping performance. Due to the shorter length, the lightship weight is also substantially decreased. Furthermore, the lightest solutions are characterized by a minimal draught and low block coefficient, further reducing the different terms in equation 7.6. Thereby, the lightship weight depends on variables similar to the ship resistance, yet a trade-off exists between lightship weight and ORI.

- Improvements in ship resistance - The Pareto-optimal design solutions allow for a reduction in ship resistance of up to 17.49%. These solutions achieve a lower ship resistance due to a shorter length, and subsequently lower frictional ship resistance. Additionally, it is that a reduction in block coefficient and draught, a typical indication of a finer hull shape, further reduces ship resistance. The opposite holds for the ORI, as the vessel with the highest ORI value shows a reduction in ship resistance compared to the base vessel. Hence, on the Pareto-front, a trade-off occurs between ship resistance and seakeeping.

The results above clearly show how the framework can efficiently explore the design space to find optimal design solutions and provide design trade-offs of conflicting requirements. In doing so, and thereby providing the Pareto frontier, the naval architect is provided with tons of useful design information. The base design, created with much deliberation by expert Naval Architects, shows the difficulty of designing a concept that maximizes performance in either one objective at once. This led to an over-dimensioned vessel design to guarantee seakeeping performance.

6. Discussion

This paper shows the advantages of using a holistic design approach for OSV design. The discussed framework can efficiently explore the concept design of OSVs, thereby effectively involving seakeeping. Specifically, it showed to be able to find substantial improvements over the base concept initially developed by C-Job. The seakeeping objective, ORI, can be increased up to 3.6%, the lightship weight decreased by 21.1% and the ship resistance decreased by 13.0%. These improvements can be achieved whilst satisfying the initial stability constraint. By being able to explore the design space early in the design process, the correct design direction can be decided. Thereby, the framework proves to be a powerful tool for the 21st-century naval architect. It should be noted that the possible design directions are still constraint by the user set boundaries, as well as possible limiting input factors such as the hull shape and loading condition. It is recommended that any naval architect carries out a sensitivity study on input parameters when applying the framework. In particular, the hull shape can significantly influence framework results. As a future development, further refining the hull shape parameters will further expand the possibilities of the framework. Caution should be applied when further developing the lightship weight and ship resistance into measures of CAPEX and OPEX. These objective values are partially determined by using reference databases. Thereby, there are inaccuracies present which may be reduced with direct analytical methods. Regardless, the framework provides a powerful tool in the arsenal of a naval architect. More precise ship design evaluation methods could be implemented as well as more parameters, constraints and objectives could be explored to further enhance the ACD framework. Thereby, C-Job's Accelerated Concept Design philosophy is further developed by applying a holistic approach accelerating the concept design process as well as generating better concepts.

Acknowledgments

This work was performed as part of the MSc thesis for the lead author, in Marine Technology at the Delft University of Technology in the assignment of C-Job Naval Architects. We would like to acknowledge both Delft University of Technology and C-Job for the support of this research.

References

AASEN, R.; BJØRHOVDE, S. (2014), *Estimating weight and CG in the early design phase*, 51, pp.13-17

ANDREWS, D. (2018), *The sophistication of early stage design for complex vessels*, Special Edition

DNV (2010), *Recommended practice: Environmental Conditions and Environmental Loads*, DNV-RP-C205, Det Norske Veritas

DE WINTER, R.; VAN STEIN, B.; DIJKMAN, M.; BÄCK, T.H.W. (2019), *Designing ships using constrained multi-objective efficient global optimization,* Machine Learning, Optimization, and Data Science

DE WINTER, R.; FURUSTAM, J.; BÄCK, T.H.W.; MULLER, T. (2020), *Optimizing Ships Using the Holistic Accelerated Concept Design Methodology*, Practical Design of Ships and Other Floating Structures (PRADS)

DE WINTER, R.; VAN STEIN, B.; BÄCK, T.H.W. (2021), *SAMO-COBRA: A Fast Surrogate Assisted Constrained Multi-objective Optimization Algorithm,* Evolutionary Multi-Criterion Optimization

GUTCH, M.; STEEN, S.; SPRENGER, F. (2020), *Operability robustness index as seakeeping performance criterion for offshore vessels*, Ocean Eng. 217

HO, C.; OKAFOR, D.; DEGREGORY, J.; TONTARSKI, N.; STOREY, T.; LIN, Z. (2012), *8520 TEU dual fuel container ship for the far east - mediterranean trade route*, 2011 - 2012 Dr. James A. Linsnyk student ship design competition

IKEDA, Y. (2014), *Prediction methods of roll damping of ships and their application to determine optimum stabilization devices,* Marine technology and SNAME news 41(02), pp.89-93

NOWACKI, H. (2010), *Five decades of computer-aided ship design,* Computer-Aided Design 42(11), pp.956-969

PAPANIKOLAOU, A. (2010), *Holistic ship design optimization,* Computer-Aided Design 42(11), pp.1028-1044

PAPANIKOLAOU, A. (2019), *A Holistic Approach to Ship Design*, Springer

PAWLING, R.; PERCIVAL, V.; ANDREWS, D. (2017), *A study into the validity of the ship design spiral in early stage ship design,* J. Ship Production and Design 33(2), pp.81-100

RIQUELME, N.; VON LÜCKEN, C.; BARAN, B. (2015), *Performance metrics in multi-objective optimization*, Latin American computing conference IEEE.

VAN DER LOOS, A.; NORMANN. H.; HANSON. J.; HEKKERT. M. (2020), *The co-evolution of innovation systems and context: Offshore wind in Norway and the Netherlands,* Renewable and Sustainable Energy Reviews

VOSSEN, C.; KLEPPE, R.; RANDI, S. (2013), *Ship design and system integration,* DMK Conf.